ORIGINAL SCIENTIFIC PAPER

CROATICA CHEMICA ACTA

Croat. Chem. Acta **2019**, *92*(2), 211–228
Published online: October 25, 2019
DOI: 10.5562/cca3540

HKD 1926

1,2-Annulated Adamantane Heterocyclic Derivatives as Anti-Influenza A Virus Agents

Vasiliki Pardali, Erofili Giannakopoulou, Athina Konstantinidi, Antonios Kolocouris, Grigoris Zoidis*

School of Health Sciences, Department of Pharmacy, Division of Pharmaceutical Chemistry, National and Kapodistrian University of Athens, Panepistimiopolis-Zografou, GR-15771 Athens, Greece

* Corresponding author's e-mail address: zoidis@pharm.uoa.gr

RECEIVED: July 1, 2019 ✶ REVISED: August 10, 2019 ✶ ACCEPTED: August 12, 2019

THIS PAPER IS DEDICATED TO PROF. KATA MLINARIĆ-MAJERSKI ON THE OCCASION OF HER 70TH BIRTHDAY

Abstract: In this report we review our results on the development of 1,2-annulated adamantane heterocyclic derivatives and we discuss the structure-activity relationships obtained from their biological evaluation against influenza A virus. We have designed and synthesized numerous potent 1,2-annulated adamantane analogues of amantadine and rimantadine against influenza A targeting M2 protein the last 20 years. For their synthesis we utilized the key intermediates 2-(2-oxoadamantan-1-yl)acetic acid and 3-(2-oxoadamantan-1-yl)propanoic acid, which were obtained by a simple, fast and efficient synthetic protocol. The latter involved the treatment of protoadamantanone with different electrophiles and a carbon-skeleton rearrangement. These ketoesters offered a new pathway to the synthesis of 1,2-disubstituted adamantanes, which constitute starting materials for many molecules with pharmacological potential, such as the 1,2-annulated adamantane heterocyclic derivatives. To obtain additional insight for their binding to M2 protein three structurally similar 1,2-annulated adamantane piperidines, differing in nitrogen position, were studied using molecular dynamics (MD) simulations in palmitoyl-oleoyl-phosphatidyl-choline (POPC) hydrated bilayers.

Keywords: 1,2-Annulated adamantane derivatives, Anti-influenza A virus agents, H3N2, H1N1, Rimantadine, Amantadine, SAR, M2 protein, POPC hydrated bilayers.

INTRODUCTION

INFLUENZA is an acute viral infection of the upper and lower respiratory tract, characterized by sudden onset of fever, cough, myalgia, malaise and other symptoms. Because of its extremely high transmissibility, influenza affects annually a large part of the world's population. Infections range from mild to severe, while pneumonia is the most common serious complication. Underlying conditions such as lung diseases, auto-immune, neurological or cardiovascular disorders, immunosuppressive therapy, diabetes and pregnancy are predisposing factors for hospitalization.[1] Seasonal influenza viruses that cause influenza in vertebrates (including birds, humans, and other mammals) are divided into types A, B, C and D,[2] and represent four of the seven genera of the *Orthomyxoviridae* family. The classification of the type of the virus is based on the antigenic specificity of the internal nucleoprotein (NP) and matrix (M) proteins.[3] Influenza D viruses primarily affect cattle and are not known to infect or cause illness in people.[2] The clinical aspects and epidemiology of influenza C virus infections are poorly characterized and rely mainly on a few studies in paediatric populations.[4] On the other hand, influenza A and B viruses circulate and affect each year approximately 5–10 % of the adult and 20–30 % of the paediatric population,[5] causing seasonal epidemics of disease with significant morbidity and mortality, particularly in high risk groups. Worldwide, annual influenza epidemics are estimated to result in about 3 to 5 million cases of severe illness, and about 290.000 to 650.000 respiratory deaths.[2] Although pandemics appear irregularly, there is always a permanent risk of a sudden influenza pandemic, such as the 'Spanish flu' in 1918,[6] the most deadly pandemic in the history of mankind, and the swine-origin H1N1 pandemic in 2009. Only influenza type A viruses are known to have caused pandemics.[7]

Influenza A Virus

As members of the *Orthomyxoviridae* family, influenza A viruses (IAV) are enveloped viruses with a segmented

negative-oriented single-stranded RNA genome. The virus particles are pleomorphic, forming usually roughly spheroidal virions with a diameter of approximately 100 nm, as well as elongated filamentous viral particles reaching over 300 nm in length.[8] Despite their pleomorphism, the viral particles comprise three basic structural characteristics; the envelope, the matrix protein (M1) and the virion core (Figure 1). The viral envelope is a lipid bilayer derived from the plasma membrane of the infected cell. The envelope contains three transmembrane proteins; hemagglutinin (HA), neuraminidase (NA) and the M2 ion channel.[9] HA and NA proteins are anchored in the lipid raft domain of the viral envelope, projecting away from the viral surface, and are the two main antigenic determinants of the virus. IAVs are further classified into subtypes depending on the genetic and antigenic properties of the hemagglutinin (HA) and neuraminidase (NA) surface glycoproteins and their combinations. To date, 18 different HA subtypes and 11 different NA subtypes are known to exist in nature.[3] Changes in the hemagglutinin and neuraminidase surface antigens are responsible for the appearance of antigenically novel strains that evade host immunity and cause reinfections.

Hemagglutinin is a homotrimeric glycoprotein and is the major envelope protein (~ 80 %). HA has a multifunctional activity as both an attachment factor and membrane fusion protein, thus mediating virus entry and infectivity.[9] NA is the second most abundant (~ 17 %) envelope protein and forms tetrameric spikes in the surface of the viral envelope. Being responsible for the release of newly formed virions from infected cells, by enzymatically cleaving the sialic acid groups from host glycoproteins, NA is required for influenza virus replication.[9] The third protein of the viral envelope, M2 ion channel, functions as a homotetramer, forming a proton-selective ion channel in the centre of four helices.[10] On average, there are ~ 16–20 ion channels in every virion,[9] nevertheless, M2 is a multifunctional protein with roles in virus entry, assembly and budding. The envelope and its three integral membrane proteins HA, NA, and M2 overlay a matrix of M1 protein, which is essential for viral integrity and encloses the virion core.

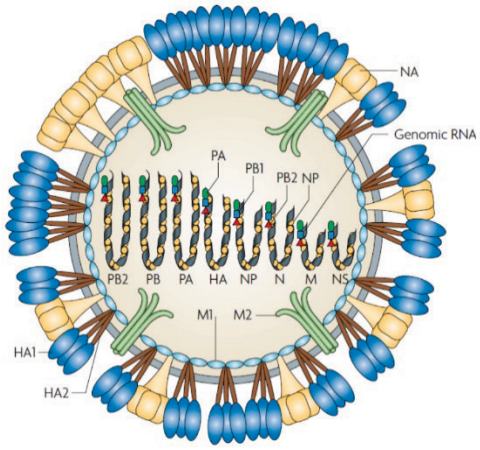

Figure 1. Structure of an influenza A virus particle.[11]

Internal to the M1 matrix, in the viral core, are found the nuclear export protein (NEP; also called nonstructural protein 2, NS2) and the helical viral ribonucleoprotein (vRNP) complexes. vRNPs comprise the eight viral RNA (vRNA) segments (PB2, PB1, PA, HA, NP, NA, M and NS genes)[12] encoding for the viral proteins. Each one of the vRNPs is bound to multiple copies of viral nucleoprotein (NP) and carries its own single, heterotrimeric RNA-dependent RNA polymerase complex (3P complex), composed of two "polymerase basic" (PB1, PB2) and one "polymerase acidic" (PA) subunits.[8,9]

The Influenza Virus Replication Cycle

IAV predominantly enters cells by endocytosis. The virion is internalized in an endosome and its acidification allows vRNPs to being released and transferred into the nucleus, where they serve as template for genome transcription and replication. Progeny vRNPs are then exported to the cytoplasm and finally trafficked to the plasma membrane for incorporation into newly forming virions. M2 and NA are the major proteins that mediate release of the virions from infected cells. M2 promotes scission of budding viruses from the plasma membrane, whereas NA prevents virus aggregation at the cell surface.[13] Therefore, there is an utmost need for new M2 inhibitors as antivirals.

Prevention and Treatment of Influenza Virus Infections

The usage of the first class of commercially anti-influenza drugs, amantadine and rimantadine (M2 proton channel blockers) has been discontinued. Since 2005, the amantadine-insensitive Ser-to-Asn mutation at position 31 in M2 (S31N) has become globally prevalent, abrogating the clinical usefulness of amantadine and possibly other previously reported M2 inhibitors due to the loss of the V27 pocket for the adamantyl cage.[14,15] The currently licensed antiviral agents for the prevention and treatment of influenza A infections are the neuraminidase inhibitors (NAIs) and the polymerase inhibitors (Figure 2). The NAIs mimic the transition-state analogue of the natural substrate of the NA enzyme, thereby blocking NA cleavage activity. Zanamivir and oseltamivir are the only two NAIs approved in most countries. Newer NAIs include laninamivir, approved in Japan, and peramivir, approved in Japan, China, South Korea, and the USA.[16] Finally, favipiravir (PB1 inhibitor), pimodivir (PB2 inhibitor), and baloxavir marboxil (PA inhibitor), that target different protein subunits of the influenza

polymerase complex are in advanced clinical development, with baloxavir being already approved in both the USA and Japan. All of the polymerase inhibitors show synergistic interactions with NAIs in preclinical models, and are orally administered.[17]

The most effective way to prevent morbidity and mortality caused by severe influenza infections is generally considered to be vaccination. However, the existing influenza vaccines fail to provide a broadly protective and long-lasting immunity and require annual updating, therefore the administration of antiviral drugs is an important first line of defense against the virus.

In this review we provide an overview of 1,2-annulated adamantane heterocyclic derivatives, synthesized by our group, which were evaluated as anti-influenza A agents and are thought to inhibit the M2 ion channel because of their structural similarities with the M2 proton channel blockers amantadine and rimantadine.

Influenza A M2 Channel – Mechanism of Action of Amantadine-Based Drugs

The M2 protein of the influenza A virus (A/M2) forms a homotetrameric acid-activated proton selective channel that is essential for several different functions during the life cycle of the virus.[18–23] When the virus enters the infected cell by endocytosis, the influenza A M2 channel is activated in response to the lowered pH of the endosome, resulting in proton flux into the virus interior, which triggers the dissociation of the viral RNA from matrix M1 protein and the fusion of the viral and endosomal membranes. After these events the viral RNA is released to the cytoplasm and replicated by the host cell.[19,24,25] In later stage of virus replication, the M2 protein maintains the high pH of the trans-Golgi network and prevents premature conformational changes of hemagglutinin in viruses with a high pH optimum of hemagglutinin-induced fusion.[26]

The M2 protein of the influenza A virus is a 97-residue single-pass membrane protein, containing a short N-terminal periplasmic domain, a transmembrane (TM) domain, and a C-terminal cytoplasmic tail.[27] Aminoadamantane (*Aamt*) class of antiviral drugs such as, amantadine (*Amt*) and rimantadine (*Rim*), have the M2 proton channel of the wild type (WT) influenza A as their primary target by blocking proton conductance through the transmembrane domain of M2 (M2TM).[28]

N-terminal domain is a highly conserved residue sequence and assists M2 incorporation into the virion,[29] however the C-terminal domain of the protein interacts with the matrix M1 protein which is necessary for virus packaging and budding.[30] Besides these two regions there is a transmembrane domain (TM, residues 23-46) comprising the pore of a proton channel with a tilt of about 25° and an amphipathic helix (AH, residues 47-62) and are essential for the functional integrity of the channel inducing the membrane curvature and membrane scission.[31] The M2TM is the minimal construct needed for tetramerization, selective proton transport and *Amt* binding, since the rate of conductance of the M2TM domain and the inhibition by the *Amt* correspond to those of the full-length protein.[14,32–35] M2TM domain accomodates the proton-conducting

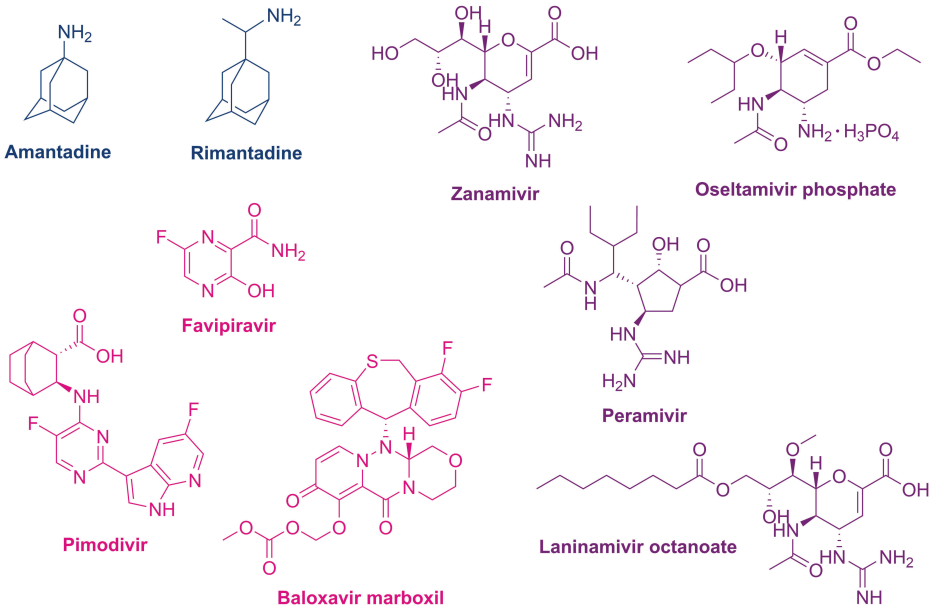

Figure 2. Chemical structures of anti-influenza agents. Zanamivir, oseltamivir, peramivir, laninamivir, and baloxavir are approved drugs.

residue, histidine 37 (His37),[36] and the channel-gating residue, tryptophan 41 (Trp41).[37] The open state of the channel is a result of the low pH in the viral endosome, when the imidazole rings of the four His37 residues are protonated causing destabilization of helix-helix packing by electrostatic repulsion. The His tetrad is located near the center of the channel acting as a pH sensor and controls the activation of the channel at pH lower than 6.0, leading ultimately to the unpacking of the influenza viral genome and to pathogenesis.[38] A secondary role for His37 is to serve as a shuttle that is sequentially protonated and deprotonated as an excess proton transits the activated channel. The side chains of Trp41 under basic conditions alter their conformation closing the C-terminal pore below His37 and form a gate that prevents proton flow through the pore.[35] The Trp41 tetrad, next to the His37 tetrad toward the C-terminus and virus interior, comprises a pH-dependent gate for proton conductance.[37] The cooperativity between the protonation state of the His37 tetrad, conformations of the protein backbone and Trp41 side chains is crucial for the pH dependent activation mechanism of the channel.[39–41] In alkaline conditions the imidazole rings of the His37 residues at Nδ1 are deprotonated[42] and the Trp41 side chains close the C-terminal pore below His37, effectively blocking proton flow though the channel. Inside the pore, ordered waters form continuous hydrogen-bonding networks that span the pore from the Val27 tetrad to His37.[43,44]

The binding site of *Amt* and *Rim* is the lumen of the four-helix bundle of the M2TM interacting with the pore-lining residues Val27, Ala30, Ser31 and Gly34 of the N-terminus portion of the M2TM.[45] The hydrophobic adamantane moiety of *Amt* or *Rim* is positioned in N-terminus on the exterior of the virus with the ammonium group directed downwards toward His37. The adamantane is located within a predominantly hydrophobic pocket formed by the side chains of Val27, Ala30 and Ser31. The hydroxyl of Ser31 forms an internal hydrogen bond to a main-chain carbonyl of Val27, increasing the effective hydrophobicity of the environment.[46] The ammonium group of the *Aamt* is stabilized due to proximal positioned waters comprising the Ala30 layer, followed by the Gly34 water layer. Placement of the drug within the pore disturbs the overall fourfold rotational symmetry, of the largely symmetrical M2 pore and its water network. The alkylammonium groups of *Amt* and *Rim* form three hydrogen bonds with water donating protons, making it impossible to form interactions with each of the four Ala30 waters maintaining the symmetry. Thus, *Aamts* are slightly tilted inside the binding site, with the ammonium group displaced away from the central axis and toward part of the Ala30 waters.[46]

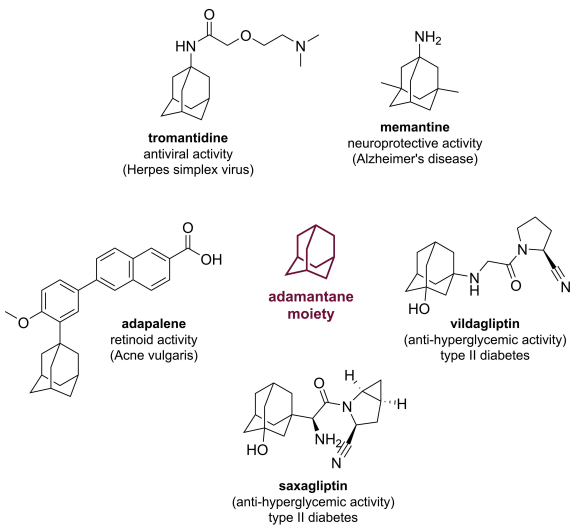

Figure 3. Currently available adamantane derivatives in clinical practice and their activity.

Adamantane as a Versatile Building Block

Generally polycyclic cage scaffolds hold a prominent place in medicinal chemistry, and they have been successfully used in drug design strategies. These cage moieties, including the adamantane ring can serve either as starting frameworks for the development of novel therapeutic agents or they can be incorporated into existing drugs to improve their pharmacokinetic and pharmacodynamic properties.[47,48]

In particular, adamantane is a rigid, almost unstrained structure of high symmetry and unique geometry. Due to its intrinsic lipophilic characteristics, it enhances the permeability of the compounds through cell membranes and facilitates the blood-brain barrier penetration. It also modulates the orientation and the binding to a hydrophobic pocket of the target in order to increase selectivity. Furthermore, its bulkiness and rigidity reduce the metabolic cleavage, thus extending the activity and the half-time of a drug.[48,49] Because of all the aforementioned, the privileged nature of the adamantane framework indicates that it constitutes a versatile building block in order to increase the drug-like properties of compounds.[50,51] Since many years, the adamantane moiety has yielded a plethora of compounds which display activity as antivirals, chemotherapeutic agents, sedatives, antihyperglycemic agents and neurotherapeutics.[52–56]

The functionalization of this scaffold is achieved by halogenation in the bridgehead positions through an easy activation of the C-H bond of the tertiary carbon atoms, giving rise to a large number of synthetic analogues with desired properties.[57]

Five drugs that feature an adamantane component are currently in clinical use (Figure 3) and many more are

under development. The approved therapeutic compounds are memantine, tromantadine, adapalene, vildagliptin and saxagliptin, and they are used to a broad spectrum of indications such as viral infections (Herpes simplex), neurodegenerative disorders (Parkinson's disease, Alzheimer's disease), acne vulgaris and type II diabetes mellitus.[58]

1,2-Annulated Adamantane Heterocycles

The first class of influenza antivirals was aminoadamantane derivatives that revolutionized the drug market (Figure 2). As previously described, the aminoadamantanes, amantadine and rimantadine, block the ion channel formed by the M2 protein of influenza A virus. All known M2 channel inhibitors are endowed with a hydrophobic scaffold, mostly an adamantane ring attached by a polar headgroup, frequently a primary or secondary amine.[57]

We, and other research groups,[59] investigated the potential of aminoadamantanyl-containing analogues as anti-influenza agents. Accordingly, we modified the headgroup to obtain M2 inhibitors with improved potency profile and explore new chemistry. To start with, we synthesized *N*-substituted analogues of rimantadine's 2-isomer,[60] which were more potent than rimantadine against influenza virus A strain H2N2. Encouraged by these preliminary results, our next approach was to attach a spiro amino substituted cycloalkane to the position 2 of the adamantane backbone, resulting in spirocyclobutane and spirocyclopentane congeners of 2-rimantadine.[60] Then, we examined the incorporation of the amino group into an heterocyclic ring and we synthesized three-, four-, and five-membered heterocycles integrated into the structure of 1-rimantadine.[61] The pyrrolidine and the azetidine counterparts exhibited activity in the order of 1.9 μM against two different influenza A strains.[61] Moreover, we introduced a spiro connection between the heterocyclic ring and the adamantane moiety[62] and the obtained spiro heterocyclic adamantane derivatives were active with EC_{50}s in the submicromolar range.

We will also review here the design, synthesis and pharmacological evaluation of 1,2-annulated adamantane heterocyclic analogues[63–65] aiming at rigidifying the conformation of the compounds to avoid binding entropic penalty and explore certain ligand binding orientations inside the M2 pore. This series of compounds (Figure 4) comprises the unsubstituted adamantanopyrrolidines **19** and **27**[63] and adamantanopiperidines **45**, **60** and **67**.[64] To explore the role of the amine nitrogen atom substitution in the anti-influenza A activity, the *N*-methyl and *N*-ethyl analogues **20**, **21**, **29**, **47**, **62**, **63** and **69** were also synthesized.[63,64] Moreover, we introduced a second amino functionality or an oxygen atom, resulting in compounds **31**, **33**, **34**,[63] **50**, **51** and **52**.[64] We also tested for their antiviral activity the highly functionalized precursors *γ*- and *δ*-lactams **15**, **16**, **18**, **26**, **28**, **44**, **58**, **59** and **66**.[63–65]

CHEMISTRY

Key Intermediates

Ketoesters and ketoacids of adamantane series are key structures for the preparation of various adamantane analogues including the 1,2 annulated adamantane

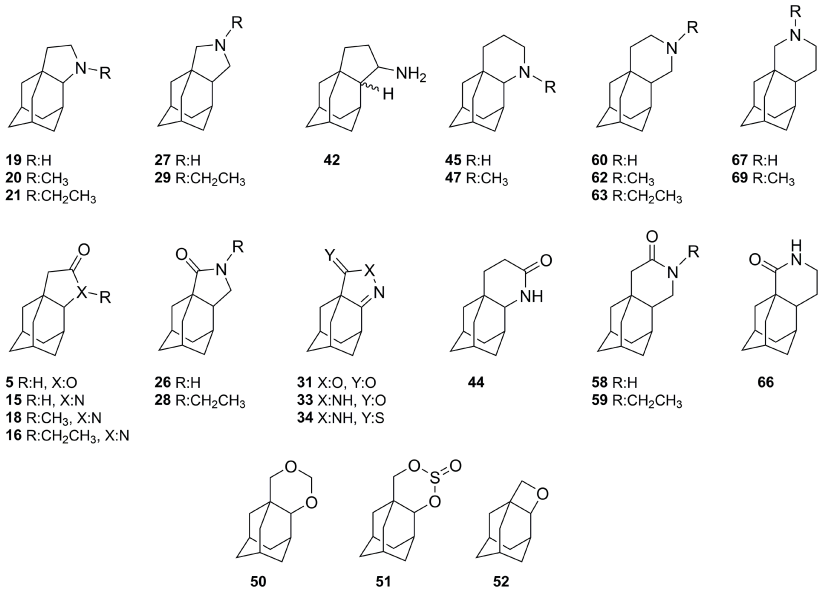

Figure 4. Structures of the 1,2-annulated adamantane derivatives described in the present study.

derivatives.[66] In general, protoadamantanone **1** constitutes basic intermediate for the 1,2-disubstituted adamantanes and it was used as starting compound for the formation of the adamantanecarboxylic acids **7** and **12**.[67] Majerski's group had described the synthesis of protoadamantanone from the commercially available 1-adamantanol since 1979.[68] 1-Adamantanol was treated with lead tetraacetate and iodine in benzene and the resulting iodo ketone was refluxed with potassium hydroxide to afford the target compound **1** in excellent yields (Scheme **1**).[68] Heating of the mixture composed of 1-adamantanol, lead tetraacetate and iodine for 2 h at 75–76 °C improved the reaction yield and decreased the amount of the unreacted starting compound.[67]

As depicted in Scheme **2**, protoadamantanone **1** was subjected to Reformatsky reaction with bromoacetic acid ethyl ester in the presence of zinc metal. Upon saponification, the hydroxyacid **2** was afforded in low yields along with some starting ketone. In an effort to obtain the derivative **2** in higher yields, protoadamantanone **1** was treated with $LiCH_2COOCH_3$, which was prepared by lithium bis(trimethylsilyl)amide and methyl ethanoate in one pot, and upon hydrolysis of the intermediate ester **3** under basic conditions, the desired compound **2** was yielded quantitatively. The hydroxyacid **2** was heated with formic acid and gave a mixture of the respective ester **4** as a major product and the lactone **5** in traces. Subsequent saponification of the mixture and Jones oxidation of the intermediate compound **6** led to the desired ketoacid **7**.[67]

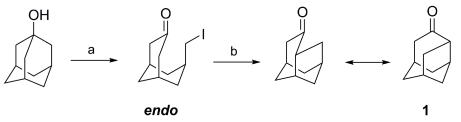

Reagents and conditions: (a) $Pb(OAc)_4$, I_2, C_6H_6, 70-75 °C (b) KOH, MeOH, reflux for 3 h.

Scheme 1. Synthesis of the starting compound protoadamantanone **1**.

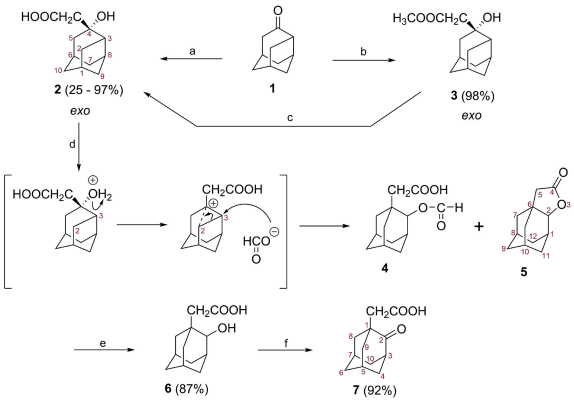

Reagents and conditions: (a) i) $BrCH_2COOEt$, Zn, C_6H_6, reflux; ii) NaOH, H_2O, EtOH, 90 °C, 2.5 h, (HCl); (b) $[(CH_3)_3Si]_2NLi$, CH_3COOCH_3, THF, –75 °C, 20 min and –60 °C, 30 min; (c) NaOH, H_2O, EtOH, 90 °C, 2.5 h, (HCl); (d) HCOOH, reflux, 30 min; (e) NaOH, H_2O, EtOH, 90 °C, 2.5 h, (HCl); (f) Jones reagent (1 M).

Scheme 2. Synthetic route to the 2-oxo-1-adamantanacetic acid building block **7**.[67]

For the preparation of the ketoacid **12** (Scheme **3**), the acetylenic diol **8** was formed by a typical Grignard reaction between protoadamantanone **1** and the dimagnesium derivative of propargylic alcohol. Catalytic hydrogenation with platinum (IV) oxide afforded the respective saturated diol **9** which was subsequently heated with formic acid to provide the corresponding diester **10**. Employment of the previously described methodology, saponification to afford the diol **11** and oxidation with Jones reagent gave the desired ketoacid **12** quantitatively.[67]

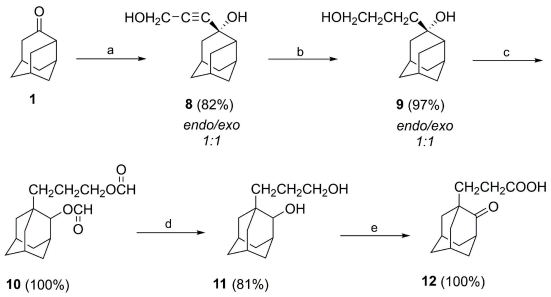

Reagents and conditions: (a) i) $BrMg-C\equiv C-CH_2OMgBr$, THF, reflux, 6 h and 24 h, 20 °C; ii) NH_4Cl, H_2O; (b) H_2, PtO_2; (c) HCOOH, reflux, 30 min; (d) NaOH, EtOH, reflux, 2 h; (e) Jones reagent (1 M).

Scheme 3. Synthetic route to the 2-oxo-1-adamantane-propionic acid building block **12**.[67]

1,2-Annulated Adamantanopyrrolidines

As illustrated in Scheme **4**, 2-oxo-1-adamantanacetic acid **7**, the synthesis of which has been described above (Scheme **2**),[67] was the key structure to afford the 1,2-annulated adamantanopyrrolidines **19**, **20** and **21**.[63,65] The ketoacid **7** was esterified with ethanol in the presence of thionyl chloride to give the ketoester **13**. The latter was converted to the respective oxime ester **14** upon reaction with hydroxylamine hydrochloride and sodium acetate. Compound **14** was hydrogenated for 10 h at 120 °C using a Raney nickel catalyst to provide the lactam **15** along with the *N*-ethyl lactam **16** in different yields. Under different hydrogenation reaction conditions, either a mixture of the lactam **16** and the amino ester **17** or the *N*-methyl lactam **18** was afforded. The amino ester **17** was refluxed in xylenes and the analogue **15** was exclusively formed. *γ*-lactams **15**, **16** and **18** were reduced to the cyclic amines **19**, **21** and **20** respectively by using lithium aluminum hydride. The *N*-methyl adamantanopyrrolidine **20** was also prepared upon *N*-acylation of the respective unsubstituted congener **19** with ethyl chloroformate and subsequent reduction of the formed carbamate **22**.[63,65]

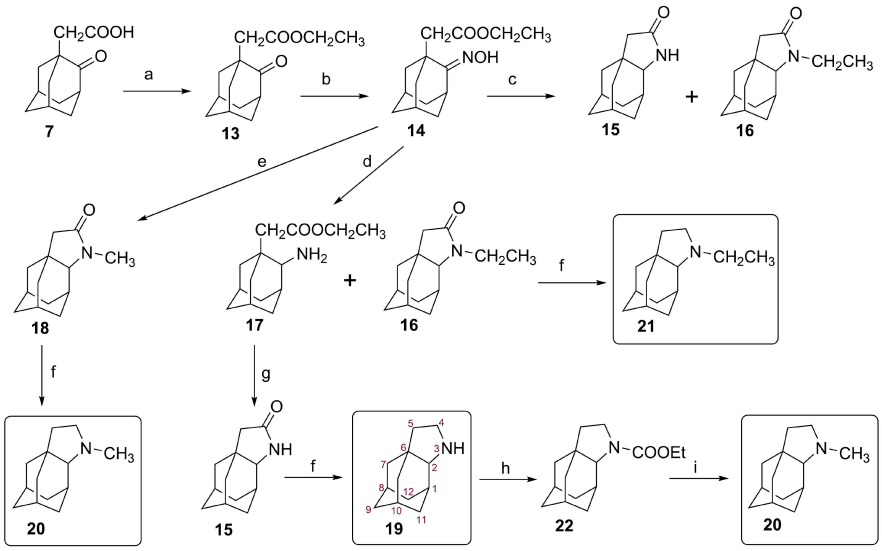

Reagents and conditions: (a) (I) $SOCl_2$, 50 °C, 30 min, (II) abs. CH_3CH_2OH (quant.); (b) $NH_2OH \cdot HCl$, $CH_3COONa \cdot 3H_2O$, $CH_3CH_2OH : H_2O$ (5 : 1), reflux, 1 h (97%); (c) (I) H_2/Ni-Raney, EtOH, 55 psi, 120 °C, 10 h, (II) xylene, reflux, 12 h (**16**: 58%, **15**: 40%); (d) H_2/Ni-Raney, EtOH, 55 psi, 100 °C, 3 h, (**16**: 23%, **17**: 34%); (e) (I) H_2/Ni-Raney, MeOH, 55 psi, 200 °C, 4 h, (II) xylene, reflux, 20 h (64%); (f) $LiAlH_4$, THF, 5 h, reflux (94-96%); (g) xylene, reflux, 12 h, (quant.); (h) Et_3N, $ClCOOCH_2CH_3$, ether, 24 h, 25 °C (96%); (i) $LiAlH_4$, THF, 24 h, 25 °C (93%).

Scheme 4. Synthesis of the 1,2-annulated adamantanopyrrolidines **19**, **20** and **21**.[63,65]

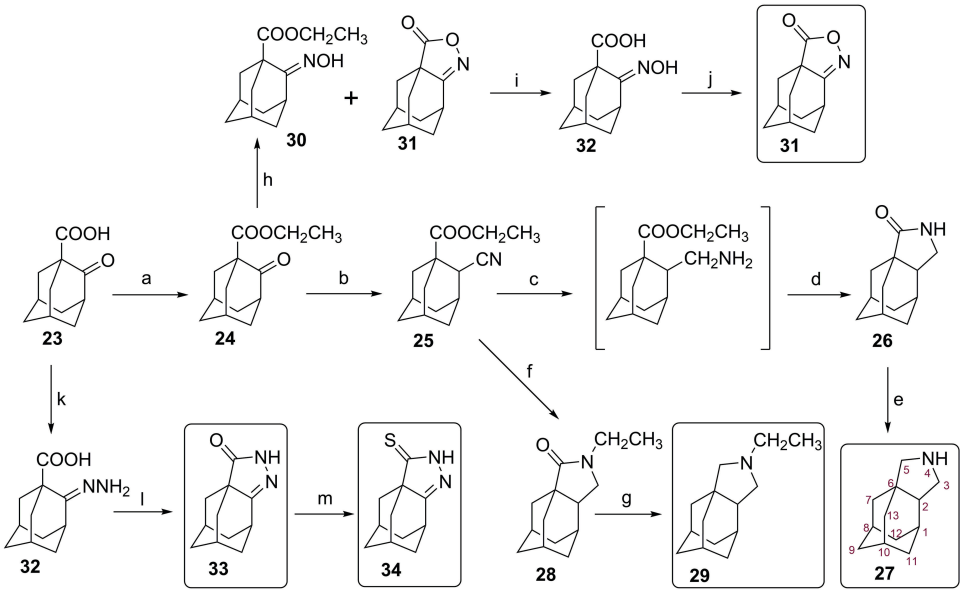

Reagents and conditions: (a) (**I**) $SOCl_2$, 65 °C, 15 min, (**II**) abs. EtOH, 1 h, rt and 30 min, 70 °C (quant.); (b) TOSMIC, abs. EtOH, DME, *t*-BuOK, 0 °C, argon, 20 °C, 30 min and 48 °C, 1 h (74%); (c) H_2/Ni-Raney, MeOH, 65 psi, 60 °C, 6 h; (d) xylene, reflux, 10 h (40%); (e) $LiAlH_4$, THF, 18 h, reflux (70%); (f) H_2/Ni-Raney, EtOH, 65 psi, 140 °C, 3 h (46%); (g) $LiAlH_4$, THF, 13 h, reflux (92%); (h) $NH_2OH \cdot HCl$, $CH_3COONa \cdot 3H_2O$, EtOH : H_2O (5 : 1), reflux, 3 h (**30**: 85%, **31**: 15%); (i) NaOH, EtOH, H_2O, 3.5 h, 60 °C and then conc. HCl (97%); (j) sublimation, 10^{-2} mmHg (79%); (k) NH_2NH_2, abs. EtOH, 30 min, reflux (72%); (l) sublimation, 10^{-2} mmHg (93%); (m) Lawesson's reagent, toluene, 12 h, reflux (93%).

Scheme 5. Synthesis of the 1,2-annulated adamantanopyrrolidines **27** and **29**, the isoxazolone **31**, the pyrazolone **33** and the pyrazolothione **34**.[63]

The synthetic routes for the annulated derivatives **27**, **29**, **31**, **33** and **34** are depicted in Scheme **5**.[63] Esterification of the 2-oxo-1-adamantane carboxylic acid **23** led to ethyl ester **24**. Reductive cyanation of the resulting ester **24** was the key step for the synthesis of the lactams **26** and **28**, which are the precursors of the target compounds **27** and **29** respectively. The use of toluenesulphonylmethyl isocyanide (TOSMIC) as nucleophile provided the cyanoester **25** in good yields. Hydrogenation of the latter by using two different sets of reaction conditions afforded the *γ*-lactams **26** and **28** which were then reduced to the desired pyrrolidine **27** and its *N*-ethyl counterpart **29** respectively.[63,65]

The ketoester **24** was coupled with hydroxylamine hydrochloride in the presence of sodium acetate, and a mixture of the oxime **30** and the oxazolone **31** was isolated. Then, the mixture was saponified and the acid oxime **32** was yielded almost quantitatively. Compound **32** was sublimed to obtain the isoxazolone **31** exclusively.[63]

The pyrazolone **33** was afforded by a two-step synthetic procedure of the ketoacid **23** with hydrazine and subsequent sublimation of the intermediate **32**. Thiation of the pyrazolone **33** with Lawesson's reagent, generated the corresponding pyrazolothione **34**.[63]

Synthesis of 1,2-Annulated Adamantane Cycloalkanamines

An example is given for compound **42**.[63] For its synthesis (Scheme **6**), the tetrahydrofuranic derivative **35** firstly reacted with the triphenyldibromophosphorane which was prepared *in situ* by addition of Br_2 to a solution of triphenylphosphine. The resulting dibromide analogue **36** was treated with sodium cyanide in DMSO to obtain a mixture of bromonitrile **37** and dinitrile **38**. The mixture was further heated in the presence of sodium cyanide in the same solvent to afford the analogue **38** in excellent yields. By employment of the Thorpe-Ziegler reaction, dinitrile **38** underwent an intramolecular condensation catalyzed by LDA to form the enamine **39**. Subsequent acid-promoted hydrolysis of the latter gave rise to the racemic cyclic ketone **40**, which was converted to the respective oxime **41** upon treatment with hydroxylamine as previously described. Compound **41** was hydrogenated over Raney nickel to provide the desired cyclopentanamine **42**.[63]

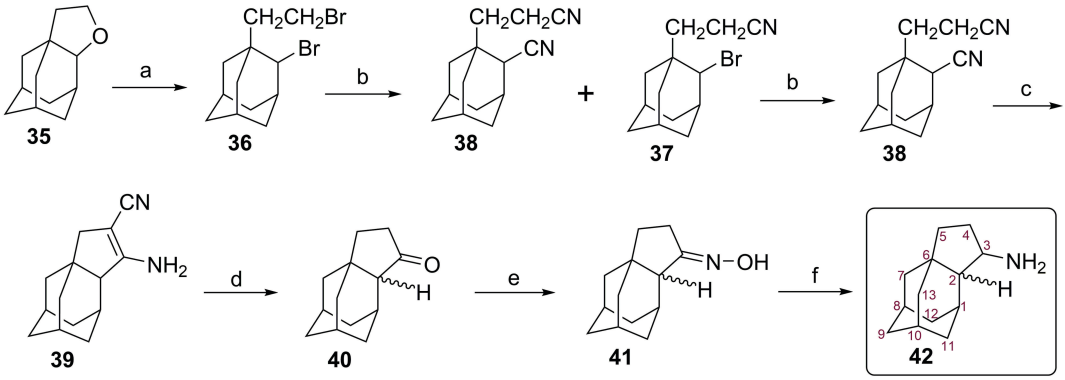

Reagents and conditions: (a) Br_2, C_6H_5CN, Ph_3P, 124 °C, 4 h, (84%); (b) NaCN, DMSO, 115 °C, 1 h and 145 °C, 1 h (**37**: 75%, **38**: 18%) and then NaCN, DMSO, 155 °C, 1 h (**38**: 89%); (c) LDA, THF, -80 °C (quant.); (d) H_2SO_4 (33%), glacial CH_3COOH, reflux, 20 h (quant.); (e) $NH_2OH \cdot HCl$, $CH_3COONa \cdot 3H_2O$, abs. EtOH : H_2O (14 : 1), 6 h, reflux (94%); (f) EtOH, Ni-Raney, 50 psi, 70 °C, 4 h (86%).

Scheme 6. Synthetic procedure for the preparation of the 1,2-annulated adamantane cyclopentanamine **42**.[63]

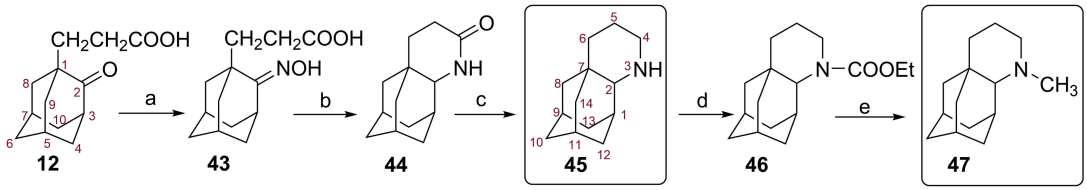

Reagents and conditions: (a) $NH_2OH \cdot HCl$, $CH_3COONa \cdot 3H_2O$, CH_3CH_2OH : H_2O (9:1), reflux, 5 h (94%); (b) H_2/Ni-Raney, EtOH, 50 p.s.i., 200 °C, 4 h (94%); (c) $LiAlH_4$, THF, 20 h, reflux (98%); (d) Et_3N, $ClCOOC_2H_5$, ether, 24 h, 25 °C (quant.); (e) $LiAlH_4$, THF, 20 h, 50 °C (96%).

Scheme 7. Synthesis of the 1,2-annulated adamantanopiperidines **45** and **47**.[64,65]

Synthesis of 1,2-Annulated Adamantanopiperidines

The formation of the piperidines **45** and **47**[64] (Scheme **7**) was achieved following a synthetic procedure similar to that of the pyrrolidines **19** and **20** (Scheme **4**). Starting from 2-oxo-1-adamantanepropionic acid **12**, the oxime **43** was afforded almost quantitatively by refluxing an ethanolic solution of the ketoacid **12** with hydroxylamine hydrochloride and sodium acetate. Compound **43** was subjected to catalytic hydrogenolysis using a Raney nickel catalyst to yield the lactam **44** which was reduced to the respective piperidine **45** using lithium aluminum hydride. The latter was *N*-acylated with ethyl chloroformate in the presence of triethylamine and the carbamate protected amine **46** was reduced to the *N*-methyl amine **47** with $LiAlH_4$.[64,65]

Piperidines **60**, **62** and **63**[64] were prepared as outlined in Scheme **8**. Protoadamantanone **1** reacted with dimethylsulfonium methylide to form the epoxide **48** as a mixture of endo/exo epimers in a 1 : 15 ratio. Oxirane ring opening under acidic conditions provided the adamantane diol **49**. Intramolecular cyclization of **49** gave the dioxane **50** in poor yields, upon heating with formaldehyde in concentrated sulfuric acid. The diol **49** was treated with thionyl chloride and afforded a reaction mixture of the dioxathiane **51** and the oxetane **52**. Compounds **51** and **52** were isolated separately after chromatographic purification. As it seems, the temperature may have a key role in the formation ratio of the two products. Traces of the cyclic sulfite **51** were detected at 43 °C. Treatment of the cyclic ether **52** with hydrobromic acid afforded the bromoalcohol **53**. The oxetane **52** was converted to the dibromide **54** as previously

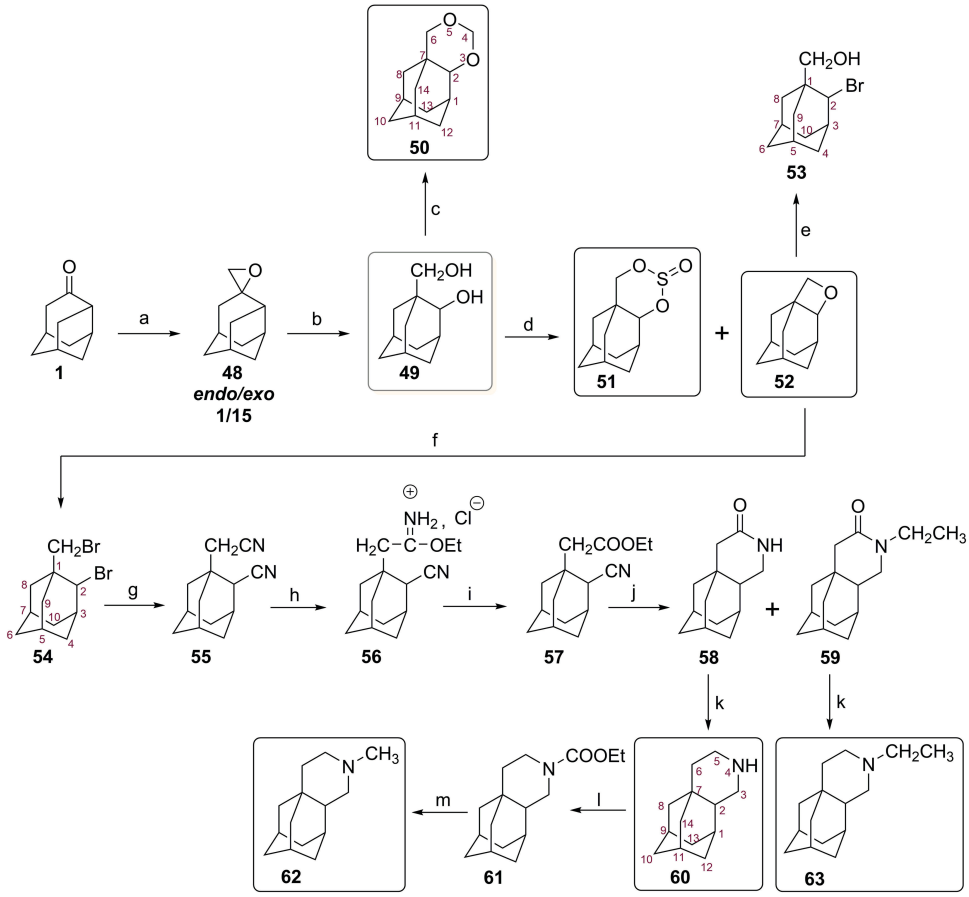

Reagents and conditions: (a) $(CH_3)_2S{=}CH_2$, DMSO, 3 h, 25 °C and 8 h, 55 °C; (b) H_2SO_4/H_2O (0.085 M), acetone; (c) HCHO, H_2SO_4, 2.5 h, 110 °C (94%); (d) (I) $SOCl_2$, Et_2O, 2.5 h, 43 °C (98%); (e) HBr, reflux, 30 min (68%); (f) Br_2, C_6H_5CN, Ph_3P, 122 °C, 4 h (38%); (g) NaCN, DMSO, 4 h, 170 °C (88%); (h) EtOH–HCl, 10 days, 30 °C (82%); (i) H_2O, HCl, ether, 24 h, 30 °C (86%); (j) H_2/Ni-Raney, EtOH, 55 p.s.i., 140 °C, 7 h (**58**: 21%, **59**: 26%); (k) $LiAlH_4$, THF, 20 h, reflux (98%); (l) Et_3N, $ClCOOC_2H_5$, ether, 24 h, 25 °C (quant.); (m) $LiAlH_4$, THF, 20 h, 50 °C (96%).

Scheme 8. Synthetic procedures for the preparation of the 1,2-annulated adamantanopiperidines **60**, **62** and **63**,[64,65] and the 1,2-annulated adamantane heterocycles **50**, **51** and **52**.[69]

described using the freshly prepared triphenyldibromophosphorane in one pot procedure.[69] The adamantane halide **54** was heated with sodium cyanide at high temperature to provide the dinitrile **55**. The latter was mixed with a saturated ethanolic solution of gaseous HCl and was left on standing for a long period of time. Mild acidic hydrolysis of the obtained imino ether hydrochloride **56** gave the cyanoester **57** which was hydrogenated using Raney nickel catalyst. The hydrogenolysis products were a mixture of the *δ*-lactams **58** and **59**. By employing the abovementioned procedure for the synthesis of piperidines **45** and **47**, reduction of the compounds **58** and **59** afforded the adamantanopiperidi-nes **60** and **63**, whereas *N*-acylation and subsequent $LiAlH_4$ catalyzed reduction of the intermediate **61** led to the *N*-methyl piperidine **62**.[64,65]

The procedure applied for the synthesis of the cyclic amines **67** and **69**[64] is illustrated in Scheme **9**. Formation of the nitrile **65** was based on the nucleophilic addition of a phosphonate-stabilized carbanion onto the ketoester **64** *via* a typical Horner-Wadsworth-Emmons reaction. Compound **64** was treated with diethyl cyanomethylphosphonate, where sodium hydride was used as a base to deprotonate the latter. The olefin **65** was appeared as a mixture of *E*/*Z* stereoisomers with excellent *E*-selectivity. Catalytic hydrogenolysis of the mixture and subsequent intramolecular cyclization provided the annulated piperidinone **66**. Conversion of the lactam **66** to the piperidine **67** was effected by reduction with $LiAlH_4$. Alkylation of the amine nitrogen atom was performed by C-N bond formation, firstly through *N*-acylation of compound **67**, followed by reduction of the intermediate **68** to afford the desired analogue **69**.[64,65]

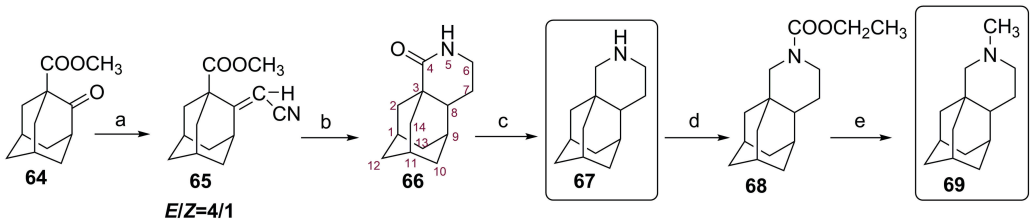

Reagents and conditions: (a) $(EtO)_2POCH_2CN$, C_6H_6, NaH, 1 h at 20 °C and then 15 min at 65 °C (95%); (b) H_2/Ni-Raney, EtOH, 50 p.s.i., 150 °C, 10 h (40%); (c) $LiAlH_4$, THF, 10 h, reflux (91%); (d) Et_3N, $ClCOOC_2H_5$, ether, 24 h, 25 °C (quant.); (e) $LiAlH_4$, THF, 20 h, 50 °C (96%).

Scheme 9. Synthesis of the 1,2-annulated adamantanopiperidines **67** and **69**.[64]

EXPERIMENTAL

Molecular Docking Calculations

The $M2TM_{WT}$-*Amt* crystal structure (PDB ID 2KQT) was used as a starting point and the *Aamt* ligands were docked using Glide (Maestro 10.3, Schrodinger, Cambridge, MA).[70] Prior to the docking calculations the 1,2-annulated adamantane piperidines **45**, **60** and **67** in their ammonium form were built by means of Maetro 10.3, prepared using the LigPrep workflow and minimized by MacroModel workflow as implemented on Maestro 10.3. N- and C-termini of the M2TM model systems were capped by acetyl and methylamino groups after applying the protein preparation module of Maestro 10.3. The structures of the protein and *Aamts* derivatives **45**, **60**, **67** were saved separately and were used for the subsequent docking calculations. The ligands were minimized using OPLS2005 force field, the polak-ribier conjugate gradient (PRCG) method and by applying a distance-dependent dielectric constant of 4.0 until a convergence value of 0.001 kJ $Å^{-1}$ mol^{-1} was reached. Docking poses of $M2TM_{WT}$-*Aamt* complexes were generated by docking the prepared compound structures into the pore binding site of the M2TM. Docking was performed with Glide XP using GlideScore multi-ligand scoring function and carried out on the energy-minimized poses. Docking poses for each ligand were virtualy inspected using Maestro workflow and the pose with the best score was used in MD simulations.

Molecular Dynamics Simulations

The $M2TM_{WT}$ complexes were simulated using the experimental structure of M2TM from Cady et al. (PDB ID 2KQT),[71] which was determined at pH 7.5 in presence of *Amt*,[71,72] as initial configuration. Each $M2TM_{WT}$ – *Aamt* complex was embedded in a hydrated membrane of POPC molecules, with the 1,2-annulated adamantane piperidine ligand in its ammonium form. The all-atom MD simulations were performed with Desmond (Schrodinger, Cambridge, MA).[46,73,74] The POPC lipid bilayer extended 20 Å beyond the solutes in x,y axes, resulting in a system including 120 lipid molecules. The bilayer was solvated using a 20 Å thick layer of TIP3P waters. The systems were neutralized by adding Na^+ and Cl^- ions in the water phase and to represent the experimental salt concentration of 0.150 M NaCl. The

total number of system's atoms reached approximately 50000. Membrane creation and system solvation were conducted with the "System Builder" utility of Desmond.[73,74] Protein-ligand interactions were modelled using OPLS2005.[75–77] The TIP3P[78] model was used for water. Calculation of long-range electrostatic interactions, was utilized by the particle mesh Ewald method,[79,80] with a grid spacing of 0.8 Å. Van der Waals and short-range electrostatic interactions were smoothly truncated at 9.0 Å. A constant temperature was maintained in all simulations using Nosé-Hoover thermostat, and the Martyna-Tobias-Klein method was employed to control the pressure.[81] Periodic boundary conditions were applied (70 × 70 × 86) Å^3. Multi-step RESPA integrator[82] was used to integrate the equations of motion with an inner time step of 2 fs for bonded interactions and non-bonded interactions within a cut-off of 9 Å. An outer time step of 6.0 fs was used for non-bonded interactions beyond the cut-off. The equilibration protocol consists of a series of restrained minimizations and MD simulations designed to relax the system, while not deviating substantially from the initial coordinates. Initially, two rounds of steepest descent minimization with a maximum of 2000 steps and harmonic restraints of 50 kcal mol^{-1} Å^{-2} were applied on all solute atoms, followed by 10000 steps of minimization without restraints. The first simulation was run for 200 ps at a temperature of 10 K in the NVT ensemble with solute heavy atoms restrained with a force constant of 50 kcal mol^{-1} Å^{-2}. The temperature was then raised during a 200 ps MD simulation to 310 K in the NVT ensemble with the force constant retained. The temperature of 310 K was used in the MD simulations in order to ensure that the membrane state is above the melting temperature state of 271 K for POPC lipids.[83] The heating was followed by equilibration runs. Three stages of NPT equilibration (1 Atmosphere) with restraints were performed, first with the heavy atoms of the system restrained for 1 ns, then with solvent and lipid molecules restrained harmonically with a force constant of 10 kcal mol^{-1} Å^{-2} for 10 ns. Finally, the third stage, with the C_α atoms of M2TM harmonically restrained with a force constant of 2 kcal mol^{-1} Å^{-2} for 1 ns. The above-mentioned was followed by a 200 ns NPT simulation without restraints. Within this time, the total energy, system dimensions, and the RMSD reached a plateau, and the systems were considered equilibrated. For structural analyses, snapshots of the different systems were created with VMD[84] or Maestro.[85] Trajectories were analyzed with Maestro, Gromacs,[86,87] and VMD. Measurements were done with Gromacs tools. For the calculation of hydrogen bonds, a cut-off angle of 30° of deviation from 180° between the donor-hydrogen-acceptor atoms and a cut-off distance of 3.5 Å between the donor and acceptor atoms were applied.

RESULTS AND DISCUSSION

The antiviral effects of the synthesized 1,2 annulated adamantane analogues **19**, **20**, **21**, **27**, **29**, **31**, **33**, **34**, **42**, **45**, **47**, **50**, **51**, **52**, **60**, **62**, **63**, **67** and **69** were determined *in vitro* against influenza A/Hong Kong/7/87 (H3N2) strain[63,64,69] and were compared to the activity of amantadine, rimantadine and ribavirin (Table 1).

The adamantane heterocycles **19**, **20**, **21**, **27**, **29**, **42**, **45**, **47**, and **67** were significantly active against influenza A virus, with EC_{50}s ranging from 0.46 to 7.70 µM. Pyrrolidine **27** and piperidine **67** were the most potent analogues with submicromolar EC_{50} values (0.46 µM and 0.6 µM, respectively). Compound **19** exhibited EC_{50} = 2.20 µM and its efficacy was comparable to that of amantadine. Incorporation of an alkyl substituent onto the nitrogen atom of the adamantanopyrrolidine **19** progressively decreased the activity of the compounds. Thus, the *N*-methyl and *N*-ethyl counterparts **20** and **21** were found to be 1.5 and 3.5-fold less potent than their parent compound **19**, respectively (EC_{50} **20** = 3.40 µM and EC_{50} **21** = 7.70 µM). It is noteworthy that shifting the nitrogen atom from position 3 to the C-4 position of the aminoadamantane heterocycle **19** increased the activity with the EC_{50} value of **27** being 5-fold lower (EC_{50} **27** = 0.46 µM). Compound **27** was 4-fold more potent compared to amantadine, almost equipotent to rimantadine and 19-fold more effective than ribavirin. A similar trend was observed for the *N*-alkylated analogue **29** (EC_{50} **29** = 2.40 µM), which was 3-fold more active than the *N*-ethyl congener **21** (EC_{50} **21** = 7.70 µM). Taking a closer look at the effect of the size of the *N*-heterocyclic ring, replacement of the pyrrolidine ring in **19** with the piperidine moiety in **45** lowered the activity by 2-fold (EC_{50} **45** = 4.1 µM), compared to derivatives **19** and **20** respectively. In the context of alkylation, the *N*-methylated analogue **47** exhibited potency similar (in the order of 4 µM) to the corresponding NH compound **45**. In contrast with the adamantanopyrrolidine analogues, moving the amine nitrogen atom from position 3 to the vicinal position resulted in a total loss of activity in the 1,2 annulated adamantanopiperidine compounds **60**, **62** and **63**. Somewhat surprisingly, the antiviral activity was regained by shifting the nitrogen atom at position 5 thus increasing the distance from the 2-adamantanyl carbon. The EC_{50} value of **67** was 7-fold lower (EC_{50} **67** = 0.6 µM) compared to the structurally related piperidine **45**. Also, compound **67** was 3-fold and 14.5-fold more potent than amantadine and ribavirin respectively. However, methylation had a detrimental effect in the potency of **67**. Changing the pyrrolidine ring in structure **19** with the isostere amino substituted cyclopentane ring in compound **42** enhanced the activity by 2-fold (EC_{50} **42** = 1.10 µM). Intriguingly,

Table 1. Anti-influenza **A** virus **(H3N2)** activity and cytotoxicity of the 1,2-annulated adamantane heterocyclic analogues **19**, **20**, **21**, **27**, **29**, **31**, **33**, **34**, **42**, **45**, **47**, **50**, **51**, **52**, **60**, **62**, **63**, **67** and **69**[(a)] in MDCK cells.[(b)]

Compound	Structure	EC_{50}[(c)(e)] / µM	MCC[(d)(e)] / µM	SI (ratio MCC/ EC_{50})	Compound	Structure	EC_{50}[(c)(e)] / µM	MCC[(d)(e)] / µM	SI (ratio MCC/ EC_{50})
19		2.20 ± 1.10	468	217	**69**	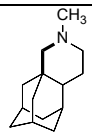	N/A[(f)]	-	-
20	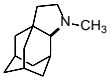	3.40 ± 2.70	439	128	**42**	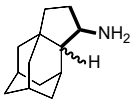	1.10 ± 1.60	88	77
21	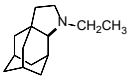	7.70 ± 2.90	83	11	**31**	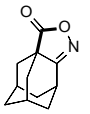	N/A[(f)]	105	< 5
27	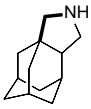	0.46 ± 0.28	94	200	**33**	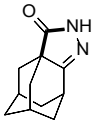	N/A[(f)]	> 525	< 5
29	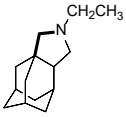	2.40 ± 1.60	83	35	**34**	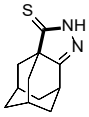	N/A[(f)]	> 525	< 5
45		4.1 ± 3.6	439	106	**50**	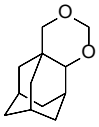	N/A[(f)]	-	-
47	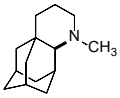	4.4 ± 2.6	83	19	**51**	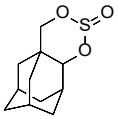	N/A[(f)]	> 250	-
60		N/A[(f)]	-	-	**52**		N/A[(f)]	> 250	-
62	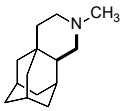	N/A[(f)]	-	-	Amantadine	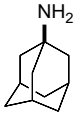	2.00	> 100	> 51
63	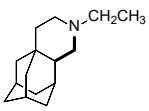	N/A[(f)]	-	-	Rimantadine	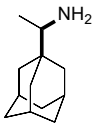	0.36	> 100	> 276
67	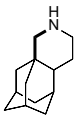	0.6 ± 0.4	439	732	Ribavirin	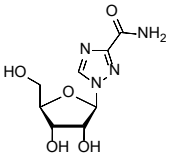	8.70	20	2

[(a)] The 1,2-annulated adamantanopyrrolidines **19**, **20**, **21**, **27** and **29**, and the adamantanopiperidines **45**, **47**, **60**, **62**, **63**, **67** and **69** were tested as hydrochlorides. Oxazolone **31**, pyrazolone **33** and pyrazolothione **34** were tested as free bases.

[(b)] MDCK, Madin-Darby canine kidney cells; virus strain: influenza A/Hong Kong/7/87 (H3N2).

[(c)] Concentration producing 50 % inhibition of the virus-induced cytopathic effect, as determined by measuring the cell viability with the colorimetric formazan-based MTS assay.

[(d)] Minimal cytotoxic concentration, or concentration that causes microscopically detectable changes in cell morphology.

[(e)] Data are shown as mean ± SD (in brackets: number of independent determinations).

[(f)] N/A: not active at subtoxic concentrations or the highest concentration tested (~500 µM).

replacement of the pyrrolidine moiety by other 5-membered heterocycles such as an isoxazolone (**31**), a pyrazolone (**33**) or a pyrazolothione (**34**) ring led to a dramatic loss of activity. Furthermore, the 1,2-annulated adamantane dioxane (**50**), dioxathiane (**51**) and oxetane (**52**) showed no inhibitory activity at the highest concentration tested (~ 500 μM). Concerning the cytotoxic effects of the compounds, the non-substituted analogues **19**, **45** and **67** and the *N*-methyl substituted pyrrolidine **20** displayed very low cytotoxicity, with MCCs in the 439-468 μM range, thus resulting in remarkable selectivity indices, which varied from 106 for **45** to 732 for **67**. It is of great interest that the introduction of an alkyl substituent onto the amine nitrogen atom of the heterocycle progressively increased the cytotoxicity of the compounds, leading to lower SI values. Finally, out of all compounds, **27** and **67** exhibited high activity and favorable selectivity (SI **27** 200; SI **67** 732).

No activity was observed for the *γ*- and *δ*-1,2 annulated adamantane lactams against influenza A/H3N2 virus, in contrast with the respective pyrrolidines and piperidines. Surprisingly, the adamantane lactam analogues retained potency in the range of 1.4–30 μM when they were evaluated for their antiviral activity against influenza A/Puerto Rico/8/34 (H1N1) strain (Table 2). Thus, lactam **15** was active with an EC_{50} value at low micromolar level. This compound was 25- and 3-fold more effective than amantadine and ribavirin respectively and its activity was comparable to that of rimantadine (EC_{50} **15** = 4.1 μM). *N*-Methyl substitution on the amide nitrogen atom of the parent compound **15** led to a 4-fold decrease in potency for the analogue **18** (EC_{50} **18** = 16 μM). Therefore, *N*-ethyl substitution on the heterocyclic ring seems to maintain antiviral activity, whereas compound **16** was equipotent (EC_{50} **16** = 5.3 μM) to the NH congener **15** (EC_{50} **15** = 4.1 μM).

Table 2. Anti-influenza A virus (H1N1) activity and cytotoxicity of the 1,2-annulated adamantane lactams **15**, **16**, **18**, **26**, **28**, **44**, **58**, **59**, **66** and of the lactone **5** in MDCK cells.[65]

Compound	Structure	Antiviral EC_{50} for influenza A/H1N1 (A/PR/8/34)[a] MTS / μM	Cytotoxicity		SI (ratio MCC / EC_{50})	Compound	Structure	Antiviral EC_{50} for influenza A/H1N1 (A/PR/8/34)[a] MTS / μM	Cytotoxicity		SI (ratio MCC / EC_{50})
			MCC[b] / μM	CC_{50}[c] / μM					MCC[b] / μM	CC_{50}[c] / μM	
15	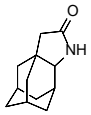	4.1	>100	>100	>24	59	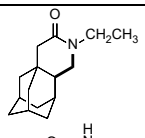	>100	>100	>100	-
18	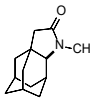	16	>100	≥ 64	>6	66	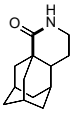	21	≥ 20	≥ 66	-
16		5.3	>100	39	>19	5	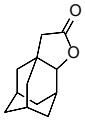	>100	≥ 20	34	-
26	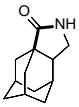	30	>100	>100	>3	Amantadine	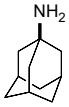	102	> 500	>500	>5
28		>100	≥ 20	36	-	Rimantadine	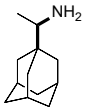	5.3	500	229	94
44		>100	>100	>100	-	Ribavirin	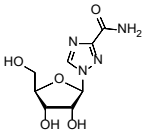	12	>100	>100	>8
58	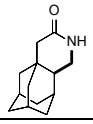	1.4	>100	≥ 77	>71						

[a] 50 % Effective concentration, or concentration causing 50 % inhibition of virus-induced cytopathic effect, as determined by measuring the cell viability with the colorimetric formazan-based MTS assay.

[b] Minimum cytotoxic concentration (MCC), i.e. concentration that causes amicroscopically detectable alteration of normal cell morphology.

[c] 50 % cytotoxic concentration (CC_{50}), as determined by measuring the cell viability with the colorimetric formazan-based MTS assay.

Table 3. Structural and dynamic measures from 200 ns MD trajectories of M2TM-Aamt ligand complexes in POPC bilayer.

Ligand	RMSD (Cα)[(a)]	Angle C-N vector[(b)]	Val27-Ad[(c)]	Ala30-Ad[(c)]	Gly34-Ad[(c)]	H-bonds[(d)]	Cl-N distance[(e)]	RMSF ligand[(f)]
45	0.8 ± 0.2	39.9 ± 8.1 (C-N)	2.1 ± 0.0	1.9 ± 0.0	2.8 ± 0.1	2.0 ± 0.2	40.2 ± 8.1	0.1
60	1.1 ± 0.2	25.7 ± 8.7 (C-N)	2.1 ± 0.0	1.9 ± 0.0	2.8 ± 0.1	1.8 ± 0.4	37.9 ± 9.2	0.1
67	1.0 ± 0.2	16.3 ± 8.0 (C-N)	2.1 ± 0.0	1.9 ± 0.0	2.8 ± 0.1	1.8 ± 0.4	40.6 ± 7.9	0.1

(a) Maximum root-mean-square deviation (RMSD) for C_α atoms of M2TM tetramer relative to the initial structure after root-mean-square fitting of C_α atoms of M2TM; in Å.

(b) Angle between the vector along the bond from the carbon atom of the adamantane core to the ligand nitrogen atom and the normal of the membrane; in degrees.

(c) Mean distance between center of mass of Val27, Ala30 or Gly34 and centers of mass of adamantane calculated using Gromacs tools; in Å.

(d) Mean number of H-bonds between ligand's ammonium group and waters.

(e) Mean distance in Å between the ligand N and the nearest Cl.

(f) Maximum root-mean-square fluctuation (RMSF) for the ligand.

Compared with amantadine, the EC_{50} of the *N*-ethyl counterpart **16** was 19-fold lower, whereas it was equipotent to rimantadine.

Moving the amide nitrogen atom from position 3 to the vicinal position of the *γ*-lactam **15** yielded compound **26** which was 7-fold less active (EC_{50} **26** = 30 μM). The same trend was observed for the analogue **28**; when increasing the distance of the amide nitrogen atom from the adamantane scaffold resulted in a substantial loss of activity for the respective *N*-ethyl congener **16**. Extension from a five- (compound **15**) to a six-membered ring (compound **44**) diminished the antiviral potency. On the other hand, shifting the nitrogen atom from C-3 to the C-4 position of the *δ*-lactam **44** provided the most potent analogue **58** of this series with an EC_{50} value of 1.4 μM. Lactam **58** was 73, 4 and 8.5 times more potent than amantadine, rimantadine and ribavirin, respectively. The presence of an ethyl group on the amide nitrogen atom of the parent compound **58** abolished the antiviral activity for the substituted derivative **59**. A further shift of the amide nitrogen atom to position 5 of the *δ*-lactam ring led to a 15-fold decrease in potency (EC_{50} **66** = 21 μM). Replacing the lactam nitrogen atom of compound **15** with an oxygen atom caused a clear reduction in activity for the respective lactone **5**.

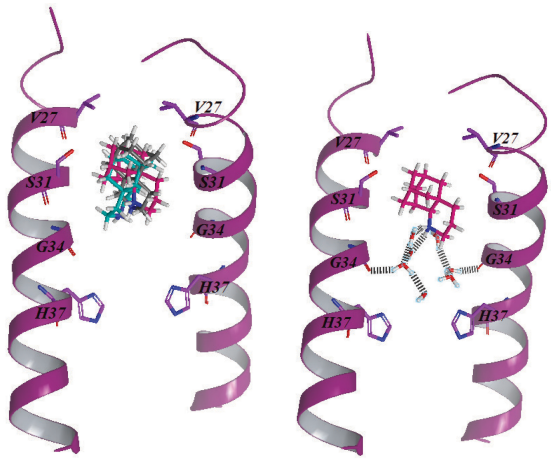

Figure 5. (*left*) Superposition of the three 1,2-annulated adamantane piperidines bound to $M2TM_{WT}$ in hydrated POPC after 200 ns of production. (*right*) Snapshot from the simulation of **45** bound to $M2TM_{WT}$ in hydrated POPC after 200 ns of production. Waters within 5 Å of the ligand define two layers of waters between the ligand's ammonium group and His37. Two hydrogen bonds between the ammonium group of the ligand and two water molecules of an upper layer close are shown. Water network that connects carbonyl groups in the protein (Gly34) together with van der Waals interactions of the adamantane core with V27 and A30 stabilize the ligand inside the pore with its ammonium group oriented towards the C-terminus.

Molecular Dynamics Simulations

To obtain additional insight and quantitatively explain the different anti-influenza virus A activity of three structurally similar 1,2-annulated adamantane piperidines[64] MD simulations were applied.

MD simulations were performed on M2TM in complex with each *Aamt* ligand in POPC hydrated bilayers. The simulated complexes were structurally stable during the 200 ns simulations with no significant conformational changes as suggested by the RMSD of C_a carbons which were smaller than 2.0 Å. The ammonium groups of the three ligands are oriented towards the C-end with a progressive increased tilt from **67** to **60** and **45** (Table 3, Figure 5). The water molecules inside the pore form two separated layers forming hydrogen bonding networks. The adamantane is embraced by the side chains of Val27 and the ammonium group forms two hydrogen bonds with the waters inside the pore (Table 3). Summarizing, the MD simulations suggest that **45**, **60**, **67** are stabilized inside the M2TM pore with no significant differences between the three 1,2-annulated adamantane piperidines.

CONCLUSION

In summary, we have designed and synthesized a series of 1,2-annulated aminoadamantane derivatives based on the structurally related M2 blockers amantadine and rimantadine. Fascinating standard chemistry enabled the synthesis of these rigid compounds with various chemical entities including pyrrolidines, piperidines with nitrogen atom at different positions of the fused ring as well as a variety of other heterocycles. Evaluation of their *in vitro* antiviral activity revealed analogues with potency against influenza A strains. Among the tested compounds, analogues **15**, **16**, **19**, **20**, **21**, **29**, **42**, **45**, **47** and **58** displayed micromolar potency in the 1.1-7.7 µM range, while compounds **27** and **67**, the most active against influenza A virus strain H3N2, were endowed with an EC_{50} < 0.6 µM and were not cytotoxic. Derivative **58** exhibited EC_{50} value up to 2 orders of magnitude lower than that of amantadine and comparable to rimantadine against influenza A/H1N1 virus. The collected data obtained from the antiviral properties of this panel of compounds allowed a preliminary interpretation of structure-activity relationships. Substitution of the free nitrogen atom either in 1,2-annulated adamantanopyrrolidines and adamantanopiperidines or in 1,2-annulated lactams was not well tolerated, and in general, the activity was decreased with increasing the alkyl chain length. Moreover, removing the nitrogen atom from position 3 to the C-4 position in the case of 1,2-annulated pyrrolidines led to more potent analogues. As concerns the 1,2-annulated adamantanopiperidines, increasing the distance from the 2-adamantanyl carbon improved the activity observed, but only in the context of shifting the amine nitrogen atom from position 3 to C-5 position. Furthermore, the incorporation of a second heteroatom into the heterocycle abolished the activity, as well the replacement of the nitrogen atom of the lactam ring by an oxygen atom. The MD simulations of the three 1,2-annulated adamantane piperidines define similar binding profile. The ammonium group participating in the formation of two hydrogen bonds with ordered waters inside the channel and the adamantane cage are located near the hydrophobic region of Val27 and Ala30. The three molecules inclined differently inside the M2TM pore in order to form hydrogen bonds with water molecules. Additional kinetic experiments using electrophysiology can account for the different potency of these molecules. Finally, this work provides an extended structure-activity relationship study, while some insight into the rational design of potential M2 inhibitors is gained for the development of antivirals with even increased activity and improved cytotoxic and resistance profile. In addition, biological studies to evaluate the ability of these functionalized aminoadamantane scaffolds to block the M2 ion channel will be of great importance including the elucidation of the exact mechanism of action.

REFERENCES

[1] N. Chauhan, J. Narang, S. Pundir, S. Singh, C. S. Pundir, *Artif. Cells Nanomed. Biotechnol.* **2013**, *41*, 189–195. https://doi.org/10.3109/10731199.2012.716063

[2] Organization, W.H.O, Influenza (Seasonal). 06/11/2018 [cited 24.06.2019]; Available from: https://www.who.int/news-room/fact-sheets/detail/influenza-(seasonal).

[3] F. Villalón-Letelier, A. G. Brooks, P. M. Saunders, S. L. Londrigan, P. C. Reading, *Viruses* **2017**, *9*, 376. https://doi.org/10.3390/v9120376

[4] N. Salez, J. Mélade, H. Pascalis, S. Aherfi, K. Dellagi, R. N. Charrel, F. Carrat, X. de Lamballerie, *J. Infect*. **2014**, *69*, 182–189. https://doi.org/10.1016/j.jinf.2014.03.016

[5] M. Carcelli, D. Rogolino, A. Gatti, L. De Luca, M. Sechi, G. Kumar, S. W. White, A. Stevaert, L. Naesens, *Sci. Rep.* **2016**, *6*, 31500. https://doi.org/10.1038/srep31500

[6] J. K. Taubenberger, D. M. Morens, *Emerg. Infect. Dis.* **2006**, *12*, 15–22. https://doi.org/10.3201/eid1201.050979

[7] R. J. Garten, C. T. Davis, C. A. Russell, B. Shu, S. Lindstrom, A. Balish, W. M. Sessions, X. Xu, E. Skepner, V. Deyde, M. Okomo-Adhiambo, L. Gubareva, J. Barnes, C. B. Smith, S. L. Emery, M. J. Hillman, P. Rivailler, J. Smagala, M. de Graaf, D. F. Burke, R. A. M. Fouchier, C. Pappas, C. M. Alpuche-Aranda, H. López-Gatell, H. Olivera, I. López, C. A. Myers, D. Faix, P. J. Blair, C. Yu, K. M. Keene, P. D. Dotson Jr., D. Boxrud, A. R. Sambol, S. H. Abid, K. St. George, T. Bannerman, A. L. Moore, D. J. Stringer, P. Blevins, G. J. Demmler-Harrison, M. Ginsberg, P. Kriner, S. Waterman, S. Smole, H. F. Guevara, E. A. Belongia, P. A. Clark, S. T. Beatrice, R. Donis, J. Katz, L. Finelli, C. B. Bridges, M. Shaw, D. B. Jernigan, T. M. Uyeki, D. J. Smith, A. I. Klimov, N. J. Cox, *Science* **2009**, *325*, 197–201. https://doi.org/10.1126/science.1176225

[8] N. M. Bouvier, P. Palese, *Vaccine* **2008**, *26*, D49–D53. https://doi.org/10.1016/j.vaccine.2008.07.039

[9] D. P. Nayak, R. A. Balogun, H. Yamada, Z. H. Zhou, S. Barman, *Virus Res.* **2009**, *143*, 147–161. https://doi.org/10.1016/j.virusres.2009.05.010

[10] T. Sakaguchi, Q. Tu, L. H. Pinto, R. A. Lamb, *Proc. Natl. Acad. Sci. U.S.A.* **1997**, *94*, 5000–5005. https://doi.org/10.1073/pnas.94.10.5000

[11] G. B. Karlsson Hedestam, R. A. Fouchier, S. Phogat, D. R. Burton, J. Sodroski, R. T. Wyatt, *Nat. Rev. Microbiol.* **2008**, *6*, 143–155. https://doi.org/10.1038/nrmicro1819

[12] P. Palese, *Cell* **1977**, *10*, 1–10. https://doi.org/10.1016/0092-8674(77)90133-7
[13] A. J. Eisfeld, G. Neumann, Y. Kawaoka, *Nat. Rev. Microbiol.* **2015**, *13*, 28–41. https://doi.org/10.1038/nrmicro3367
[14] A. L. Stouffer, R. Acharya, D. Salom, A. S. Levine, L. Di Costanzo, C. S. Soto, V. Tereshko, V. Nanda, S. Stayrook, W. F. DeGrado, *Nature* **2008**, *451*, 596–599. https://doi.org/10.1038/nature06528
[15] R. M. Pielak, K. Oxenoid, J. J. Chou, *Structure* **2011**, *19*, 1655–1663. https://doi.org/10.1016/j.str.2011.09.003
[16] L. V. Gubareva, T. G. Besselaar, R. S. Daniels, A. Fry, V. Gregory, W. Huang, A. C. Hurt, P. A. Jorquera, A. Lackenby, S. K. Leang, J. Lo, D. Pereyaslov, H. Rebelo-de-Andrade, M. M. Siqueira, E. Takashita, T. Odagiri, D. Wang, W. Zhang, A. Meijer, *Antiviral Res*. **2017**, *146*, 12–20. https://doi.org/10.1016/j.antiviral.2017.08.004
[17] F. G. Hayden, N. Shindo, *Curr. Opin. Infect. Dis.* **2019**, *32*, 176–186. https://doi.org/10.1097/QCO.0000000000000532
[18] S. D. Cady, W. Luo, F. Hu, M. Hong, *Biochemistry* **2009**, *48*, 7356–7364. https://doi.org/10.1021/bi9008837
[19] I. V. Chizhmakov, F. M. Geraghty, D. C. Ogden, A. Hayhurst, M. Antoniou, A. J. Hay, *J. Physiol.* **1996**, *494*, 329–.336 https://doi.org/10.1113/jphysiol.1996.sp021495
[20] T.I. Lin, C. Schroeder, *J. Virol.* **2001**, *75*, 3647–3656. https://doi.org/10.1128/JVI.75.8.3647-3656.2001
[21] J. A. Mould, J. E. Drury, S. M. Frings, U. B. Kaupp, A. Pekosz, R. A. Lamb, L. H. Pinto, *J. Biol. Chem.* **2000**, *275*, 31038–31050. https://doi.org/10.1074/jbc.M003663200
[22] L. H. Pinto, L. J. Holsinger, R. A. Lamb, *Cell* **1992**, *69*, 517–528. https://doi.org/10.1016/0092-8674(92)90452-I
[23] K. Shimbo, D. L. Brassard, R. A. Lamb, L. H. Pinto, *Biophys. J.* **1996**, *70*, 1335–1346. https://doi.org/10.1016/S0006-3495(96)79690-X
[24] R. A. Lamb, L. J. Holsinger, L. H. Pinto in *Cellular Receptors for Animal Viruses*, (Eds.: E. Wimmer), Cold Spring Harbor Press: Cold Spring Harbor Laboratory Press, Plainview, NY, **1994**, pp. 303–321.
[25] J. Hu, R. Fu, K. Nishimura, L. Zhang, H. X. Zhou, D. D. Busath, V. Vijayvergiya, T. A. Cross, *Proc Natl Acad Sci U.S.A.* **2006**, *103*, 6865–6870. https://doi.org/10.1073/pnas.0601944103
[26] R. J. Sugrue, G. Bahadur, M. C. Zambon, M. Hall-Smith, A. R. Douglas, A. J. Hay, *EMBO J.* **1990**, *9*, 3469–3476. https://doi.org/10.1002/j.1460-2075.1990.tb07555.x
[27] R. A. Lamb, S. L. Zebedee, C. D. Richardson, *Cell* **1985**, *40*, 627–633. https://doi.org/10.1016/0092-8674(85)90211-9
[28] L. H. Pinto, R. A. Lamb, *Mol. Biosyst.* **2007**, *3*, 18–23. https://doi.org/10.1039/B611613M
[29] E. K. Park, M. R. Castrucci, A. Portner, Y. Kawaoka, *J. Virol.* **1998**, *72*, 2449–2455.
[30] M. F. McCown, A. Pekosz, *J. Virol.* **2006**, *80*, 8178–8189. https://doi.org/10.1128/JVI.00627-06
[31] J. S. Rossman, X. Jing, G. P. Leser, R. A. Lamb, *Cell* **2010**, *142*, 902–913. https://doi.org/10.1016/j.cell.2010.08.029
[32] K. C. Duff, R. H. Ashley, *Virology* **1992**, *190*, 485–489. https://doi.org/10.1016/0042-6822(92)91239-Q
[33] C. Ma, A. L. Polishchuk, Y. Ohigashi, A. L. Stouffer, A. Schön, E. Magavern, X. Jing, J. D. Lear, E. Freire, R. A. Lamb, W. F. DeGrado, L. H. Pinto, *Proc Natl Acad Sci U.S.A.* **2009**, *106*, 12283–12288. https://doi.org/10.1073/pnas.0905726106
[34] D. Salom, B. R. Hill, J. D. Lear, W. F. DeGrado, *Biochemistry* **2000**, *39*, 14160–14170. https://doi.org/10.1021/bi001799u
[35] R. Liang, J. M. J. Swanson, J. J. Madsen, M. Hong, W. F. DeGrado, G. A. Voth, *Proc Natl Acad Sci U.S.A.* **2016**, *113*, E6955–E6964. https://doi.org/10.1073/pnas.1615471113
[36] C. Wang, R. A. Lamb, L. H. Pinto, *Biophys. J.* **1995**, *69*, 1363–1371. https://doi.org/10.1016/S0006-3495(95)80003-2
[37] Y. Tang, F. Zaitseva, R. A. Lamb, L. H. Pinto, *J. Biol. Chem.* **2002**, *277*, 39880–39886. https://doi.org/10.1074/jbc.M206582200
[38] A. Helenius, *Cell* **1992**, *69*, 577–578. https://doi.org/10.1016/0092-8674(92)90219-3
[39] R. Acharya, V. Carnevale, G. Fiorin, B. G. Levine, A. L. Polishchuk, V. Balannik, I. Samish, R. A. Lamb, L. H. Pinto, W. F. DeGrado, M. L. Klein, *Proc Natl Acad Sci U.S.A.* **2010**, *107*, 15075–15080. https://doi.org/10.1073/pnas.1007071107
[40] J. K. Williams, Y. Zhang, K. Schmidt-Rohr, M. Hong, *Biophys. J.* **2013**, *104*, 1698–1708. https://doi.org/10.1016/j.bpj.2013.02.054
[41] M. Sharma, M. Yi, H. Dong, H. Qin, E. Peterson, D. D. Busath, H. X. Zhou, T. A. Cross, *Science* **2010**, *330*, 509–512. https://doi.org/10.1126/science.1191750
[42] F. Hu, W. Luo, M. Hong, *Science* **2010**, *330*, 505–508. https://doi.org/10.1126/science.1191714
[43] J. L. Thomaston, M. Alfonso-Prieto, R. A. Woldeyes, J. S. Fraser, M. L. Klein, G. Fiorin, W. F. DeGrado, *Proc Natl Acad Sci U.S.A.* **2015**, *112*, 14260–14265. https://doi.org/10.1073/pnas.1518493112
[44] J. L. Thomaston, R. A. Woldeyes, T. Nakane, A. Yamashita, T. Tanaka, K. Koiwai, A. S. Brewster, B. A.

Barad, Y. Chen, T. Lemmin, M. Uervirojnangkoorn, T. Arima, J. Kobayashi, T. Masuda, M. Suzuki, M. Sugahara, N. K. Sauter, R. Tanaka, O. Nureki, K. Tono, Y. Joti, E. Nango, S. Iwata, F. Yumoto, J. S. Fraser, W. F. DeGrado, *Proc Natl Acad Sci U.S.A.* **2017**, *114*, 13357–13362. https://doi.org/10.1073/pnas.1705624114

[45] X. Jing, C. Ma, Y. Ohigashi, F. A. Oliveira, T. S. Jardetzky, L. H. Pinto, R. A. Lamb, *Proc Natl Acad Sci U.S.A.* **2008**, *105*, 10967–10972. https://doi.org/10.1073/pnas.0804958105

[46] J. L. Thomaston, N. F. Polizzi, A. Konstantinidi, J. Wang, A. Kolocouris, W. F. DeGrado, *J. Am. Chem. Soc.* **2018**, *140*, 15219–15226. https://doi.org/10.1021/jacs.8b06741

[47] T. P. Stockdale, C. M. Williams, *Chem. Soc. Rev.* **2015**, *44*, 7737–7763. https://doi.org/10.1039/C4CS00477A

[48] C. J. Van der Schyf, W. J. Geldenhuys, *Neurotherapeutics* **2009**, *6*, 175–186. https://doi.org/10.1016/j.nurt.2008.10.037

[49] G. Lamoureux, G. Artavia, *Curr. Med. Chem*. **2010**, *17*, 2967–2978. https://doi.org/10.2174/092986710792065027

[50] M. A. Gunawan, J.-C. Hierso, D. Poinsot, A. A. Fokin, N. A. Fokina, B. A. Tkachenko, P. R. Schreiner, *New J. Chem.* **2014**, *38*, 28–41. https://doi.org/10.1039/C3NJ00535F

[51] N. Basarić, K. Molčanov, M. Matković, B. Kojić-Prodić, K. Mlinarić-Majerski, *Tetrahedron* **2007**, *63*, 7985–7996. https://doi.org/10.1016/j.tet.2007.05.066

[52] W. J. Geldenhuys, S. F. Malan, J. R. Bloomquist, A. P. Marchand, C. J. Van der Schyf, *Med. Res. Rev.* **2005**, *25*, 21–48. https://doi.org/10.1002/med.20013

[53] J. Veljković, L. Uzelac, K. Molčanov, K. Mlinarić-Majerski, M. Kralj, P. Wan, N. Basarić, *J. Org. Chem.* **2012**, *77*, 4596–4610. https://doi.org/10.1021/jo3002479

[54] M. Sekutor, K. Mlinarić-Majerski, T. Hrenar, S. Tomić, I. Primožič, *Bioorg. Chem.* **2012**, *41-42*, 28–34. https://doi.org/10.1016/j.bioorg.2012.01.004

[55] M. Horvat, L. Uzelac, M. Marjanović, N. Cindro, O. Franković, K. Mlinarić-Majerski, M. Kralj, N. Basarić, *Chem. Biol. Drug Des*. **2012**, *79*, 497–506. https://doi.org/10.1111/j.1747-0285.2011.01305.x

[56] N. Basarić, M. Sohora, N. Cindro, K. Mlinarić-Majerski, E. De Clercq, J. Balzarini, *Arch Pharm (Weinheim)* **2014**, *347*, 334–340. https://doi.org/10.1002/ardp.201300345

[57] L. Wanka, K. Iqbal, P. R. Schreiner, *Chem. Rev*. **2013**, *113*, 3516–3604. https://doi.org/10.1021/cr100264t

[58] J. Liu, D. Obando, V. Liao, T. Lifa, R. Codd, *Eur. J. Med. Chem*. **2011**, *46*, 1949–1963. https://doi.org/10.1016/j.ejmech.2011.01.047

[59] (a) N. Kolocouris, G. B. Foscolos, A. Kolocouris, P. Marakos, N. Pouli, G. Fytas, S. Ikeda, E. De Clercq, *J. Med. Chem.* **1994**, *37*, 2896–2902; https://doi.org/10.1021/jm00044a010
(b) N. Kolocouris, A. Kolocouris, G. B. Foscolos, G. Fytas, J. Neyts, E. Padalko, J. Balzarini, R. Snoeck, G. Andrei, E. De Clercq, *J. Med. Chem*. **1996**, *39*, 3307–3318; https://doi.org/10.1021/jm950891z
(c) I. Stylianakis, A. Kolocouris, N. Kolocouris, G. Fytas, G. B. Foscolos, E. Padalko, J. Neyts, E. De Clercq, *Bioorg. Med. Chem. Lett*. **2003**, *13*, 1699–1703; https://doi.org/10.1016/S0960-894X(03)00231-2
(d) C. Fytas, A. Kolocouris, G. Fytas, G. Zoidis, C. Valmas, C. F. Basler, *Bioorg Chem.* **2010**, *38*, 247–251; https://doi.org/10.1016/j.bioorg.2010.09.001
(e) E. Torres, R. Fernández, S. Miquet, M. Font-Bardia, E. Vanderlinden, L. Naesens, S. Vázquez, *ACS Med Chem Lett.* **2012**, *3*, 1065–1069; https://doi.org/10.1021/ml300279b
(f) J. Wang, C. Ma, J. Wang, H. Jo, B. Canturk, G. Fiorin, L. H. Pinto, R. A. Lamb, M. L. Klein, W. F. DeGrado, *J. Med. Chem.* **2013**, *56*, 2804–2812; https://doi.org/10.1021/jm301538e
(g) C. Tzitzoglaki, A. Wright, K. Freudenberger, A. Hoffmann, I. Tietjen, I. Stylianakis, F. Kolarov, D. Fedida, M. Schmidtke, G. Gauglitz, T. A. Cross, A. Kolocouris, *J. Med. Chem.* **2017**, *60*, 1716–1733; https://doi.org/10.1021/acs.jmedchem.6b01115
(h) M. Barniol-Xicota, S. Gazzarrini, E. Torres, Y. Hu, J. Wang, L. Naesens, A. Moroni, S. Vázquez, *J. Med. Chem*. **2017**, *60*, 3727–3738. https://doi.org/10.1021/acs.jmedchem.6b01758

[60] G. Zoidis, N. Kolocouris, G. B. Foscolos, A. Kolocouris, G. Fytas, P. Karayannis, E. Padalko, J. Neyts, E. De Clercq, *Antivir. Chem. Chemother.* **2003**, *14*, 153–164. https://doi.org/10.1177/095632020301400305

[61] G. Zoidis, C. Fytas, I. Papanastasiou, G. B. Foscolos, G. Fytas, E. Padalko, E. De Clercq, L. Naesens, J. Neyts, N. Kolocouris, *Bioorg. Med. Chem*. **2006**, *14*, 3341–3348. https://doi.org/10.1016/j.bmc.2005.12.056

[62] N. Kolocouris, G. Zoidis, G. B. Foscolos, G. Fytas, S. R. Prathalingham, J. M. Kelly, L. Naesens, E. De Clercq, *Bioorg. Med. Chem. Lett*. **2007**, *17*, 4358–4362. https://doi.org/10.1016/j.bmcl.2007.04.108

[63] G. Zoidis, A. Tsotinis, N. Kolocouris, J. M. Kelly, S. R. Prathalingam, L. Naesens, E. De Clercq, *Org. Biomol. Chem.* **2008**, *6*, 3177–3185. https://doi.org/10.1039/b804907f

[64] G. Zoidis, N. Kolocouris, L. Naesens, E. De Clercq, *Bioorg. Med. Chem*. **2009**, *17*, 1534–1541. https://doi.org/10.1016/j.bmc.2009.01.009

[65] G. Zoidis, L. Naesens, E. De Clercq, *Monatsh. Chem.* **2013**, *144*, 515–521. https://doi.org/10.1007/s00706-013-0924-8

[66] E. A. Shokova, V. V. Kovalev, *Russ. Chem. Rev.* **2011**, *80*, 927–951. https://doi.org/10.1070/RC2011v080n10ABEH004177

[67] N. Kolocouris, G. Zoidis, C. Fytas, *Synlett.* **2007**, *7*, 1063–1066. https://doi.org/10.1055/s-2007-973899

[68] Z. Majerski, Z. Hamersak, *Org. Synth.* **1979**, *59*, 147–151. https://doi.org/10.15227/orgsyn.059.0147

[69] G. Zoidis, D. Benaki, V. Myrianthopoulos, L. Naesens, E. De Clercq, E. Mikros, N. Kolocouris, *Tetrahedron Lett.* **2009**, *50*, 2671–2675. https://doi.org/10.1016/j.tetlet.2009.03.132

[70] Schrödinger, Maestro 9.3, User Manual. 2012, New York, NY: Schrödinger Press, LLC.

[71] S. D. Cady, K. Schmidt-Rohr, J. Wang, C. S. Soto, W. F. DeGrado, M. Hong, *Nature* **2010**, *463*, 689–692. https://doi.org/10.1038/nature08722

[72] J. Hu, T. Asbury, S. Achuthan, C. Li, R. Bertram, J. R. Quine, R. Fu, T. A. Cross, *Biophys. J.* **2007**, *92*, 4335–4343. https://doi.org/10.1529/biophysj.106.090183

[73] K. J. Bowers, E. Chow, H. Xu, R. O. Dror, M. P. Eastwood, B. A. Gregersen, J. L. Klepeis, I. Kolossvary, M. A. Moraes, F. D. Sacerdoti, J. K. Salmon, Y. Shan, D. E. Shaw, in *Proceedings of the 2006 ACM/IEEE conference on Supercomputing* **2006**, ACM: Tampa, Florida. p. 84.

[74] Schrodinger, L., Maestro-Desmond Interoperability Tools, version 3.1. 2012.

[75] W. L. Jorgensen, D. S. Maxwell, J. Tirado-Rives, *J. Am. Chem. Soc.* **1996**, *118*, 11225–11236. https://doi.org/10.1021/ja9621760

[76] G. A. Kaminski, R. A. Friesner, J. Tirado-Rives, W. L. Jorgensen, *J. Phys. Chem. B*. **2001**, *105*, 6474–6487. https://doi.org/10.1021/jp003919d

[77] R. C. Rizzo, W. L. Jorgensen, *J. Am. Chem. Soc.* **1999**, *121*, 4827–4836. https://doi.org/10.1021/ja984106u

[78] W. L. Jorgensen, J. Chandrasekhar, J. D. Madura, R. W. Impey, M. L. Klein, *J. Chem. Phys.* **1983**, *79*, 926–935. https://doi.org/10.1063/1.445869

[79] U. Essmann, L. Perera, M. L. Berkowitz, T. Darden, H. Lee, L. G. Pedersen, *J. Chem. Phys.* **1995**, *103*, 8577–8593. https://doi.org/10.1063/1.470117

[80] T. Darden, D. York, L. Pedersen, *J. Chem. Phys.* **1993**, *98*, 10089–10092. https://doi.org/10.1063/1.464397

[81] G. J. Martyna, D. J. Tobias, M. L. Klein, *J. Chem. Phys.* **1994**, *101*, 4177–4189. https://doi.org/10.1063/1.467468

[82] D. D. Humphreys, R. A. Friesner, B. J. Berne, *J. Phys. Chem*. **1994**, *98*, 6885–6892. https://doi.org/10.1021/j100078a035

[83] R. Koynova, M. Caffrey, *Biochim. Biophys. Acta.* **1998**, *1376*, 91–145. https://doi.org/10.1016/S0304-4157(98)00006-9

[84] W. Humphrey, A. Dalke, K. Schulten, *J. Mol. Graph.* **1996**, *14*, 33–38. https://doi.org/10.1016/0263-7855(96)00018-5

[85] Schrodinger, L., Maestro, version 8.5. 2008.

[86] H. J. C. Berendsen, D. van der Spoel, R. van Drunen, *Comput. Phys. Commun.* **1995**, *91*, 43–56. https://doi.org/10.1016/0010-4655(95)00042-E

[87] B. Hess, C. Kutzner, D. van der Spoel, E. Lindahl, *J. Chem. Theory Comput.* **2008**, *4*, 435–447. https://doi.org/10.1021/ct700301q.